Proceedings of ICRC 2001: 1101 © Copernicus Gesellschaft 2001

ICRC 2001

Potential of AMANDA-II in HE neutrino astrophysics

S. W. Barwick, for the AMANDA collaboration

University of California - Irvine, Irvine, CA 92697 USA

Complete author list is found at the end of this volume.

Abstract. AMANDA-II, the second phase of the AMANDA program to detect high energy neutrinos from astrophysical sources was completed in February, 2000 and has taken data routinely since that time. About one year later, during the next Antarctic campaign, detector calibration studies were performed. This paper outlines the scientific program of the AMANDA-II detector and describes the potential contribution to each goal. Detector performance, such as the effective area as a function of muon energy and zenith angle and angular resolution, is used to estimate the minimum detectable flux for several specialized analysis procedures. Assuming several years of livetime, AMANDA-II has the capability to observe neutrino fluxes from diffuse and point sources that are at least an order of magnitude below current limits, and in the case of diffuse sources, reach background limited operation for neutrino energies below $\sim 10^2$ TeV. The time-integrated effective volume for muon neutrino detection is expected to reach 1 km^{3}yr for $E_\nu > 10^2$ TeV. Atmospheric neutrinos will provide a high statistics calibration of the detector performance from zenith to near the horizon. At EHE energies, the muons produced by ν_μ interactions can be differentiated from atmospheric muons. The exposure of AMANDA-II approaches 1 km^{2}yr for $E_\mu > 10^8$ TeV.

1 Introduction

The second phase of the AMANDA detector, AMANDA-II, consisting of 19 strings and 677 optical sensors (OMs), was completed in February 2000 and calibrated between December 2000 and January 2001. The OMs for physics analysis are located between 1500m to 2000m beneath the surface of the South Pole in Antarctica. The nine new strings of AMANDA-II are arranged in a circular pattern when viewed from the surface, 200m in diameter, and concentric with the initial 10 strings of AMANDA. The new strings increase the geometric area of the array and improve the technical performance of the system by incorporating new technologies for signal transmission using high-bandwidth optical cables. One string includes technology(Goldschmidt, 2001) that digitizes signals *in situ*, and transfers information over electrical cables by standard digital communication techniques. Additional information on the performance, operation, and description of the AMANDA-II detector can be found in these proceedings(Wischnewski, 2001).

The primary science objective of the AMANDA-II neutrino telescope is the search for astrophysical sources of high energy neutrinos. The science reach depends on the response of the detector to signal events and is limited by poorly reconstructed atmospheric muons and intrinsic backgrounds due to atmospheric neutrinos. The response of the detector is related to the effective area of the detector, A_{eff}, which depends on the muon energy, E_μ. Fig. 1 presents a preliminary assessment of A_{eff}, for neutrino-induced muons (i.e., upward-traveling muons) with $E_\mu = 10$ TeV at their closest approach to the center of the detector. The trigger A_{eff} of the detector, defined by the majority logic trigger implemented in hardware, exceeds 10^5 m^2. Independent of the physics objective, the ultimate sensitivity to ν-induced muons with $E_\mu = 10$ TeV cannot exceed the sensitivity inferred from this curve. The curves labeled "Am-II GRB Cuts" and "Am-II Point Cuts" show A_{eff} expected for analysis criteria optimized to search for Gamma Ray Bursts (GRB) and continuous emission from point sources, respectively. Clearly, the achievable sensitivity depends on the scientific goal. Those objectives with relatively small background, such as transient emission from a known direction in the sky, can be probed with a significant fraction of the trigger area.

The bottom two curves compare A_{eff} for AMANDA-II and AMANDA-B10 (the first phase of the detector, consisting of 10 strings and 302 optical sensors) for similar analyses. For B10, there is rather strong decrease near the horizon, which is a consequence of inadequate background rejection for horizontal muons traversing the narrow region of instrumented volume. For AMANDA-II, the slight increase

Correspondence to: S. W. Barwick
(barwick@cosmic.pdf.uci.edu)

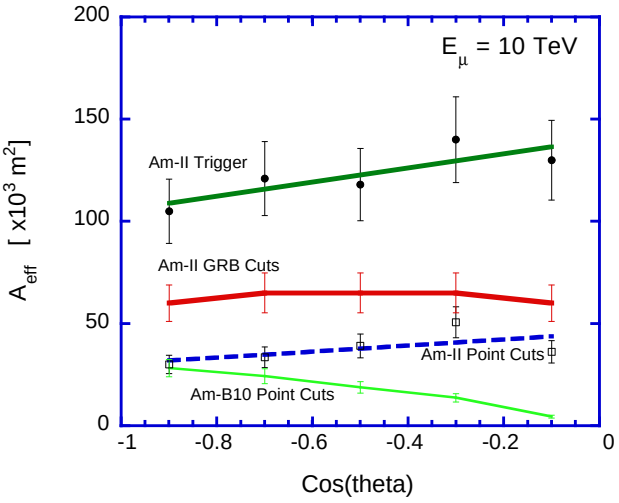

Fig. 1. Effective area of AMANDA-II as function cos(zenith) for $E_\mu = 10$ TeV at the distance of closest approach to the detector. See text for explanation of the labeled curves. Cos(zenith)=-1 indicates the direction for vertical upgoing events. Statistical errors are shown.

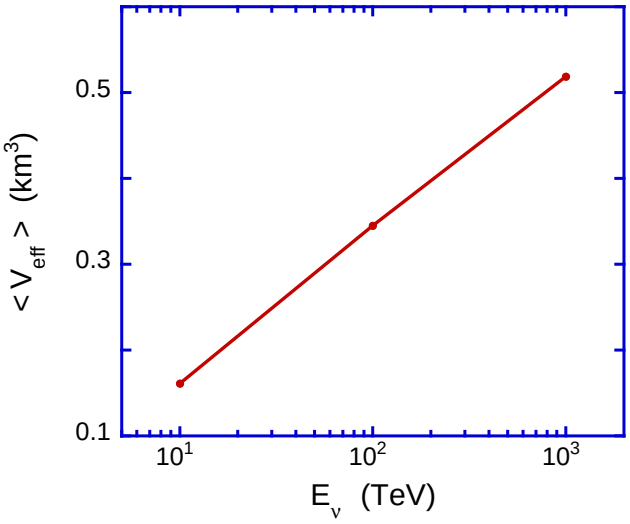

Fig. 2. Average effective volume of AMANDA-II as a function of neutrino energy. The effective volume for CC ν_μ interactions, averaged over the upgoing hemisphere, was obtained after application of the analysis procedure to search for point sources.

in A_{eff} toward the horizon for the trigger and point source curves reflects the tall cylindrical geometry of AMANDA-II. At the energy shown, the angular acceptance of AMANDA-II is much improved compared to AMANDA-B10.

The muon effective area was determined using the simulation package, AMASIM, developed for AMANDA-B10 and extended to include the response of the analog (mostly) optical OMs on nine additional strings of AMANDA-II. While AMANDA-II is physically larger than AMANDA-B10, the low energy response was de-emphasized initially to decrease the sensitivity to atmospheric background and reduce the deadtime of the data acquisition system. However, specialized, string-based trigger conditions were implemented in January 2001 to improve the performance at low energy while minimizing the impact on deadtime. Finally, $A_{eff}(E_\mu)$ should increase as the understanding of the detector improves. For example, many of the selection parameters are inappropriate for the larger detector.

A gaussian fit of the distribution for $\Delta\theta = \theta_{reco} - \theta_{MC}$ yields $\sigma_{\Delta\theta} = 1.6^\circ$, where θ_{reco} is the reconstructed zenith angle and θ_{MC} is the true zenith angle. The simulation assumed an input spectrum proportional to E^{-2}.

The effective volume for ν_μ detection by AMANDA-II is shown in Fig. 2, although the reader should keep in mind the preliminary nature of the current state of AMANDA-II analysis. The time integrated value approaches 1 km^{3}yr for $E_\nu > 10^2$ TeV after several years of operation. The implication is obvious for searches for ν_τ and ν_e neutrino flavors, which are usually detected by cascades contained within the instrumented volume. Non- observation of ν_μ signal by AMANDA-II places severe constraints on the detection rate of ν_τ and ν_e neutrino flavors.

2 Anticipated Flux Sensitivity of AMANDA-II

Since the scientific goals and associated energy spectra of signal and background are diverse, analysis methods are tailored to the physics objective, which impacts the detection efficiency as a function of energy. For example, the diffuse source analysis was designed to maximize the sensitivity to relatively hard spectra (e.g, E^{-2}). We adopted the non-optimized analysis procedures developed for AMANDA-B10 and assumed atmospheric neutrinos provide the only source of background events to estimate the minimum detectable flux.

2.1 Flux Sensitivity: Diffuse Sources

Representative predictions, upper bounds, and experimental data for a diffuse flux of high energy neutrinos are shown in Fig. 3. The dotted horizontal lines represent an estimate of the minimum detectable flux for the AMANDA-II and IceCube detectors based on their anticipated sensitivities. The atmospheric ν flux (solid curve) is averaged over angle. The dashed curve for atmospheric ν takes energy resolution into account, assumed to be characterized by a log normal distribution. The region to the right of the vertical line indicates the onset of significant attenuation by the earth.

Fig. 3 indicates that the search for continuous diffuse emission is constrained at low energies by the atmospheric neutrino background and at high energies by the absorption of the earth. At energies beyond 10^7 GeV, the search for ν_μ in the downgoing direction is preferred. The sensitivity of AMANDA- II is adequate to cover most of the observable window after 2-3 years of livetime.

While the theoretical predictions in Fig. 3 are differential, the experimental flux limits should be interpreted with

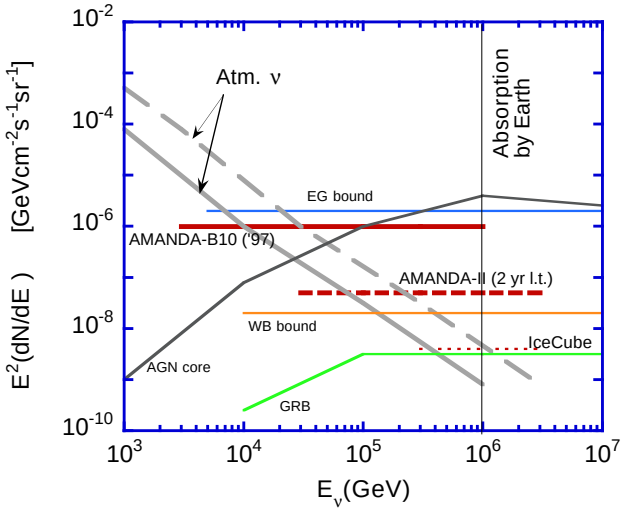

Fig. 3. Diffuse Flux: Representative survey of theoretical ν_μ-flux predictions and experimental limits for diffusely distributed sources. Models: GRB(WB, 1997), AGN core(SS, 1996), and atm. ν (Agrawal, 1996). Upper bounds: EG bound(Mannheim, 2001) and WB bound(WB, 1999). AMANDA-B10 preliminary limit(Andres, 2000) and IceCube expectation(Spiering, 2001) rescaled to 1 year.

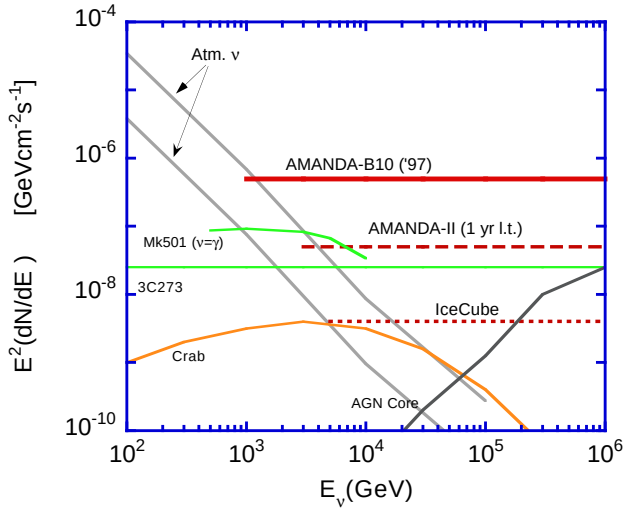

Fig. 4. Point Source: Representative survey of theoretical ν_μ flux predictions and experimental limits. AMANDA-B10 result taken from Young (2001). The dotted horizontal lines present preliminary estimates of the minimum detectable flux for the AMANDA-II and IceCube detector(Spiering, 2001). The atmospheric neutrino fluxes(Agrawal, 1996) were computed for circular bins of 1^o (lower) and 3^o radius. The upper atmospheric-ν curve is also equivalent to the curve for the 1^o sky bin after taking into account the effect of neutrino energy resolution. Models: 3C273(Nellen, 1993), Crab(BP, 1997), and AGN core(SS, 1996). Curve Mk501 assumes that the neutrino spectrum follows the measured gamma ray spectrum during its flaring phase(Weekes, 2000).

caution. For the assumed E^{-2} spectrum, the minimum detectable flux produces of order 10 events per year in the source bin. Unless energy-dependent selection criteria are imposed, the majority of detected neutrino events have energies between $10^2 - 10^4$ GeV . Therefore, energy resolution becomes a critical concern since the energy dependence of the atmospheric-ν background is very steep.

2.2 Flux Sensitivity: Point Sources

Fig. 4 shows the expected sensitivity of AMANDA-II to point sources after one year of livetime. The AMANDA-II limits were obtained by applying the point source analysis developed for AMANDA-B10, and by assuming atmospheric neutrinos generate background events, which dominate at the lowest observable energies. The sensitivity improves linearly with time if low energy events are removed by the analysis procedure. The atmospheric ν flux Φ_ν^{atm} is shown for a circular bin of 3^o radius(left curve, appropriate for AMANDA-II), and 1^o circular bin (appropriate for IceCube). The rightmost curve includes the effect of finite energy resolution for $\log(\delta E_\nu/E_\nu) \sim 0.45$, which convolves δE_μ and uncertainties associated with the distance to the interaction vertex. The search for continuous sources is limited to $10^4 < E_\nu < 10^7$ GeV. The atmospheric neutrino background limits the search for continuous sources to $E_\nu > 3\times10^3$ GeV . Of course, the background for episodically recurring or transient sources is proportionally less, but flux sensitivity improves slowly with the extension of the energy window to lower energies if the source spectrum is $\sim E^{-2}$. The sensitivity of AMANDA-II is compared to the B10 limit(Young, 2001) and a few representative models. The detection of Mk501 is hampered by the effect of finite energy resolution. However, the measured photon spectrum may be significantly softer than the neutrino spectrum due to reprocessing near the core of the source or due to absorption by intergalactic photon fields.

For AMANDA-II, the minimum integrated flux above 1 TeV is 5×10^{-11} cm^{-2}s^{-1}, which is slightly below the gamma flux limits from a recent all-sky survey(Wang, 2001). The largest integral flux emitted from a known HE gamma sources is $\sim 10^{-11}$ cm^{-2}s^{-1} for $E_\gamma > 1.5$ TeV, during the flaring phase of Mk501(Weekes, 2000). Thus, AMANDA-II can probe ν/γ ratios as small as five in HE gamma sources.

3 Gamma Ray Bursts (GRBs)

A widely discussed version of a relativistic fireball model predicts high energy neutrino emission from GRBs, which depends on the relative ratio of protons and electrons in the fireball. This parameter can be estimated by assuming that the GRBs are the source of the observed cosmic ray flux at the most extreme energies(Waxman, 1995). Shocks responsible for gamma rays also accelerate protons to relativistic energies(WB, 1997). Subsequent interactions between protons and $\sim$ MeV photons produce neutrinos with $E_\nu > 10^2$ TeV. At these energies, neutrinos should produce distinct

signatures in AMANDA, which has been the focus of current analysis(Hardke, 2001). Recently, Meszaros and Waxman(MW, 2001) predict a significant flux of neutrinos at energies greater than a few TeV from the pre-cursor to the burst. In this scenario, a neutrino burst may not be accompanied by an observable signal in gamma rays. Without an optical trigger, experimental detection is more difficult. However, the observation of 2 or more neutrinos from the same direction within a short time span can be differentiated from atmospheric background, even without an electromagnetic trigger.

With coincident gamma emission, the experimental search for neutrino emission from a GRB is greatly simplified because the cosmic ray background is dramatically reduced if the burst time and direction is obtained from another detector. The atmospheric neutrino background flux is diffusely distributed in direction and uniform in time, according to $\Phi_\nu^{atm} \sim 10^{-7} E_{\nu,TeV}^{-2.5}$ cm^{-2}s^{-1}sr^{-1}. Atmospheric background in a source bin localized with an uncertainty in the space angle of Ψ deg and restricted to a search window of t seconds relative to the onset of gamma emission is given by $F_\nu \sim 3 \times 10^{-11} (\Psi/deg)^2 (t/sec) E_{\nu,TeV}^{-2.5}$ cm^{-2}. Since the intrinsic background is undetectable, the sensitivity improves linearly with the number of bursts in the sample. Moreover, Fig. 1 suggests that $A_{eff} \sim 0.5 A_{eff}^{trig}$. Fortunately, BATSE was (briefly) operational after AMANDA-II was commissioned, so several 10's of triggers are available for study. Non-observation of neutrino emission would constrain possible variation of model parameters, such as the bulk Lorentz motion, Γ, total fireball energy, and distance(AHH, 2000). In the future, the ground-based gamma ray observatory, MILAGRO, which can search for GRBs with fluence sensitivity comparable to BATSE(Smith, 2001), will complement satellite observations.

4 EHE Physics Capability

Neutrinos with $E_\nu > 10^3$ TeV are strongly absorbed by the earth, so the usual technique to search for astrophysical sources of ν_μ in the upgoing direction becomes less appropriate. However, at these energies, AMANDA can differentiate ν_μ from atmospheric backgrounds in the *downgoing* direction(Hundertmark, 2001). Above $E_\mu \sim 10^4$ TeV, atmospheric muon and neutrino fluxes are small and the signature from EHE muons is spectacular. Since $E_\mu \sim 0.7 - 0.8 E_\nu$ for charged-current interactions at these energies, the average range of the muon exceeds the 2/cos(θ_z) kmwe overburden (except near the horizon), which limits the angle averaged V_{eff} for the detector to $\sim$4 km^3.

5 Future Directions

Next season, modifications to the AMANDA data acquisition electronics will improve the integrated dynamic range capabilities. For detectors embedded in a medium with non-negligible scattering, as is the case with AMANDA, the spread in the arrival time of the Cherenkov photons becomes much larger than the intrinsic timing resolution of the PMT (the sensing element in the AMANDA array). Under these conditions, the waveform structure produced by the PMTs for HE muon and cascade events can be quite complex. Approximately 50 channels of waveform recorders will be installed to evaluate the improvement to energy and angular resolution. In addition, new electronics will provide high quality information from existing string of digital OMs, which complements the waveform-enhanced optical channels by recording waveforms every 12m in depth.

AMANDA-II will play an important role during the construction phase of the proposed IceCube detector since the first strings will be located around the AMANDA-II site. Combining results from AMANDA-II and IceCube will enable the neutrino sky to be probed with increasing precision during the construction of IceCube.

Acknowledgements. The author acknowledges support from the U.S. National Science Foundation Physics Division and UC-Irvine AENEAS Supercomputer Facility.

References

A. Goldschmidt, et al., ICRC 2001, these proceedings.
R. Wischnewski, et al., ICRC 2001, these proceedings.
E. Waxman and J. Bahcall, Phys. Rev. Lett. 78(1997)2292.
F. W. Stecker and M. H. Salamon, Sp. Sci. Rev. 75(1996)341.
V. Agrawal, T. Gaisser, P. Lipari, and T. Stanev, Phys. Rev. D53(1996)1314.
K. Mannheim, 2001 [astro-ph/0104165].
E. Waxman and J. Bahcall, Phys. Rev. D59(1999)023002.
E. Andres, et al., Nucl. Phys.B (Proc. Suppl. Neutrino 2000) 91(2001)423.
C.Spiering, et al., 2001, these proceedings.
L. Nellen, K. Mannheim, and P.L. Biermann, Phys. Rev. D47(1993)5270.
W. Bednarek and R.J. Protheroe, Mon.Not.Roy.Astro.Soc. 287(1997)560.
T. Weekes, 2000 [astro-ph/0010431].
S. Young, UC-Irvine dissertation, 2001.
K. Wang, et al., 2001 [astro-ph/0103353].
E. Waxman, Astrophys. J.452(1995)L1; E.Waxman, Phys. Rev. Lett.75(1995)386.
R. Hardke, et al., 2001, these proceedings.
P. Meszaros and E. Waxman, 2001 [astro-ph/0103275].
J. Alvarez-Muniz, F. Halzen, and D. Hooper, Phys. Rev. D62(2000)093015.
A. J. Smith, et al., 2001, these proceedings.
S. Hundertmark, et al., ICRC 2001, these proceedings.